Journal of Computer Assisted Tomography
22(3):487–491

Visualization of the Cervical Spinal Cord with FDG and High-Resolution PET

Yoko Kamoto, Norihiro Sadato, Yoshiharu Yonekura, Tatsuro Tsuchida, Hidemasa Uematsu, Atsuo Waki, Kenzo Uchida, Hisatoshi Baba, Shinichi Imura, and Junji Konishi

Purpose: Our aim was to evaluate the visibility of the cervical spinal cord with [^{18}F]2-fluoro-2-deoxyglucose (FDG) and a high-resolution PET scanner and to quantify the glucose utilization by the cervical cord.

Method: Twenty-one normal subjects and three cervical myelopathy patients were studied. The visibility of the cervical spinal cord in sagittal and coronal sections was evaluated. The metabolic rate of glucose (MRGlu) and standardized uptake value (SUV) of FDG in the cord were calculated.

Results: The entire cervical spinal cord was clearly visualized in 57% of the subjects: the upper cord in 81%, the middle cord in 73%, and the lower cord in 57%. The MRGlu of the normal cord was 1.93 ± 0.37 mg/100 g/min. SUV was constant across all the vertebral levels and negatively correlated with subject age. In the myelopathy patients, the SUV of the entire cervical cord was lower than in the age-matched normal subjects.

Conclusion: These preliminary results indicate that the cervical spinal cord can be visualized as a normal structure in routine head and neck PET imaging and that FDG-PET may provide quantitative information about spinal cord disorders.

Index Terms: Spinal cord—Spinal cord, anatomy—Fluorodeoxyglucose (FDG)—Emission computed tomography (PET)—Spinal cord, abnormalities.

The application of PET, to investigation of the spine has been limited to the evaluation of spinal cord tumors. Several investigators (1–3) have reported the usefulness of PET with [^{18}F]2-fluoro-2-deoxyglucose (FDG) or [^{11}C]methionine for visualization and grading of cervical cord tumors and for differentiation between cancer recurrence and radiation necrosis. However, the normal spinal cord has not been studied extensively. In 1983 Di Chiro et al. (4) reported metabolic imaging of the brainstem and cervical spinal cord of normal volunteers by using PET and FDG, but the cervical spinal cord was described only above the C4 level. As a result of improvements in PET devices, delineation of normal structures in the extracranial head and neck with FDG has now become possible, and PET is currently frequently being used to evaluate neoplasms in this area (5).

From the Department of Nuclear Medicine, Kyoto University Faculty of Medicine, Kyoto (Y. Kamoto and J. Konishi), and Biomedical Imaging Research Center (N. Sadato, Y. Yonekura, T. Tsuchida, H. Uematsu, and A. Waki) and Department of Orthopaedic Surgery (K. Uchida, H. Baba, and S. Imura), Fukui Medical School, Fukui, Japan. Address correspondence and reprint requests to Dr. Y. Kamoto at Department of Nuclear Medicine, Kyoto University Faculty of Medicine, 54 Shogoinkawahara-cho, Sakyo-ku, Kyoto, 606-01, Japan.

The purpose of the present study was to investigate the characteristics of the cervical spinal cord as a part of the CNS by quantifying glucose utilization by the cord. First, we evaluated the visibility of the normal cervical spinal cord in routine FDG-PET imaging in the head and neck region. Second, the normal range of glucose utilization was evaluated by kinetic and nonkinetic approaches. Its relation to age was also investigated because glucose utilization by the normal brain tends to decrease with age (6) and because age-associated atrophic changes in the spinal cord have also been reported (7). Finally, the cervical spinal cord of myelopathy patients was evaluated in comparison with age-matched controls.

MATERIALS AND METHODS

Twenty-one subjects (12 men and 9 women, mean age 62.8 years, range 31–88 years) who underwent FDG-PET studies to evaluate tumors in the head and neck region outside the CNS were collected as a normal group. All had normal findings on a neurological examination. The cervical spinal cord and bony canal depicted by MRI and CT were normal. Thirteen of the 21 subjects underwent PET once before receiving chemotherapy or

radiation therapy. Eight subjects underwent PET studies twice, once before and once after the anticancer therapy. The interval between the two consecutive PET scans was 3 weeks to 3 months. Seven of the eight subjects received both chemotherapy and radiation therapy and one received chemotherapy alone. The chemotherapy was performed by intraarterial or intravenous infusion of a combination of carboplatin, fluorouracil, and pirarubicin. The radiation field did not include the spinal cord. Three patients with cervical myelopathy due to chronic compression by a soft and/or hard disk at only one vertebral level were also evaluated by FDG-PET. All subjects were studied under fasting conditions for at least 4 h. No diabetic patients were included. Informed consent was obtained from each subject before the PET study.

A GE Advance system (GE-YMS, Tokyo, Japan) was employed to perform the PET scanning. The physical characteristics of this scanner have been described in detail by De Grado et al. (8). This system permits simultaneous acquisition of 35 transverse slices with an interslice spacing of 4.25 mm with septa (2D mode). Images were reconstructed to FWHM of 4.2 mm in both the transaxial and the axial directions. The field of view and pixel size of the reconstructed images were 256 and 2 mm, respectively. Transmission scans were obtained for 10 min using a standard $^{68}Ge/^{68}Ga$ pin source for attenuation correction of the emission images. Approximately 244–488 MBq of FDG was injected intravenously over a 10 s period. The emission scans were performed in the following two manners according to the protocol for evaluation of tumors in the head and neck region. (a) In 23 examinations, 20 min static scans were started at 40–80 min after the intravenous injection of FDG. No arterial sampling was performed. (b) In six examinations, dynamic scans were obtained up to 60 min after the FDG injection with arterial sampling. Arterial blood was sampled manually from the radial artery on the side opposite the injection site. Starting at the time of the injection, 2 ml of blood was sampled every 15 s during the first 2 min and then at 2.5, 3, 5, 10, 15, 20, 30, 45, and 60 min after the injection. Plasma radioactivity was measured with a scintillation counter with which the PET camera had been cross-calibrated, using a cylindrical phantom filled with the ^{18}F solution.

The PET scanning was performed in the three myelopathy patients in the same manner as in the normal subjects in the second protocol.

The visibility of the cervical spinal cord with FDG-PET was evaluated in sagittal and coronal sections. First, an image-processing software (Dr. View; Asahi Kasei Joho System Co., Tokyo, Japan) was used to reconstruct sagittal and coronal images from the original transaxial images. The cervical spinal cord was then divided into three segments according to the vertebral levels, as upper (C1–3), middle (C4–5), and lower (C6–7) segments, based on the MR or CT images. The visibility of the cord was evaluated by two observers using a five grade scale for each segment. Grade 2 or greater was considered "visualized." The visualized cords were selected for quantitative analysis. A 10.3 mm diameter (21 pixels) circular region of interest (ROI) was placed in every transaxial slice of the cord. Sagittal images were used as an on-line guide to correctly position the ROI. The lower vertebral slices were often eliminated from the ROI analysis because of artifacts created by the shoulder.

The maximal count in the ROI was adopted as tissue radioactivity to eliminate the partial volume effect caused by the slightly larger size of the ROI than the diameter of the spinal cord (7). The measured maximal radioactivity of each ROI was averaged over several slices within each segment of the cord to represent the mean value of the upper, middle, and lower segments.

The standardized uptake value (SUV) of FDG was calculated as follows: SUV = tissue activity/(injected FDG dose/body wt).

The metabolic rate of glucose (MRGlu) was calculated using the Sokoloff three compartment model (9) and an autoradiographic method with a priori estimates of the rate constants and lumped constant of normal cerebral gray matter (10). When the lower cerebellum was included in the field of view, its SUV was also calculated to compare it with that of the cervical cord.

SUV and MRGlu are expressed as means ± SD. The difference in SUVs due to segment levels was evaluated by one way repeated measures analysis of variance. The difference in SUVs due to visibility scores was analyzed by one way factorial analysis of variance with a post hoc Scheffé test. Pearson and Spearman correlation coefficients were applied to the other analyses. Significance was defined as $p < 0.05$.

RESULTS

Normal Subjects

Qualitative Analysis

The normal cervical spinal cord was clearly depicted in both the sagittal and the coronal sections (Fig. 1). The visibility scores of the normal subjects' cervical spinal cord are shown in Table 1. The upper cervical cord was visualized in 81% of the subjects, the middle cord in 73%, and the lower cord in 57%, and the entire cervical cord was clearly visualized in 57%. Whenever the cord was poorly visualized, the whole image was unclear, probably because of a motion artifact. Gray and white matter could not be distinguished in sagittal, coronal, or axial images.

Quantitative Analysis

There was no significant correlation between the visibility scores and the SUV (Fig. 2). In the normal subjects, the mean SUVs of the upper, middle, and lower segments were 1.99, 1.93, and 1.91, respectively, showing a tendency toward a slight decline according to the level, but the differences did not reach statistical signifi-

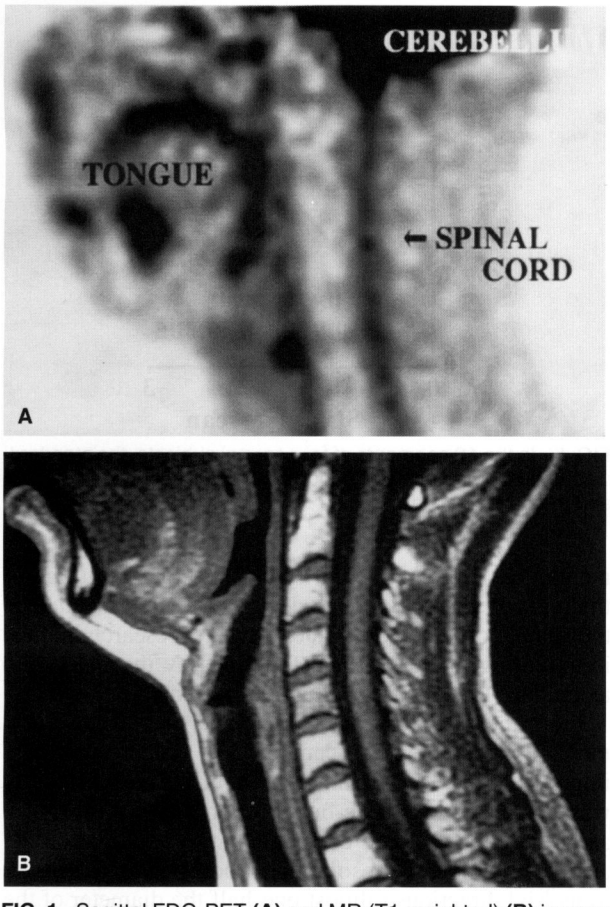

FIG. 1. Sagittal FDG-PET **(A)** and MR (T1-weighted) **(B)** images of a normal subject (30 years old).

cance (Fig. 3). The mean SUV of all three segments (entire cervical cord) was 1.95 ± 0.30. There was a negative correlation between the SUV and the age of the normal subjects (Fig. 4). The cervical cord was well depicted in four of the eight normal subjects who underwent PET examinations twice. SUVs obtained in the two examinations were similar, indicating good SUV reproducibility (Fig. 5). SUVs of the cerebellar cortex were obtained in 15 subjects, and the ratio of the SUV of the cervical cord to the SUV of cerebellum was 0.32 ± 0.05. There was no significant correlation between SUV and plasma glucose level (r = –0.397, p = 0.116, n = 17) or between SUV and time between the injection and scan (r = –0.279, p = 0.237, n = 20). The MRGlu was available in four of the six normal subjects whose arterial blood was sampled. The mean MRGlu in the four normal subjects was 1.93 ± 0.37 (Table 2). SUV tended to be positively correlated with MRGlu in the present study.

TABLE 1. *The visibility scores of the normal subjects' cervical spinal cords*

Grade	upper (C1–3) (n = 26)*	middle (C4–5) (n = 29)*	lower (C6–7) (n = 28)*
4 (excellent)	14	14	11
3 (good)	5	6	2
2 (fair)	2	1	3
1 (poor)	5	4	3
0 (none)	0	4	9
visibility (2–4)	21 (81%)	21 (73%)	16 (57%)

* The total score differed in each segment, because the field of view in the transaxial direction was decided according to the location of the tumor, which did not always cover the whole cervical cord.

Myelopathy Patients

The entire cervical spinal cord was visible in all three myelopathy patients. There was no significant localized decrease or increase in MRGlu or SUV around the compression. Instead, SUVs averaged over the entire cord of the three patients were lower than in the age-matched normal subjects (Table 2; Fig. 4).

DISCUSSION

Adequacy of Selection of Normal Population

In this study subjects suffering from non-CNS head and neck neoplasms were regarded as having a "nor-

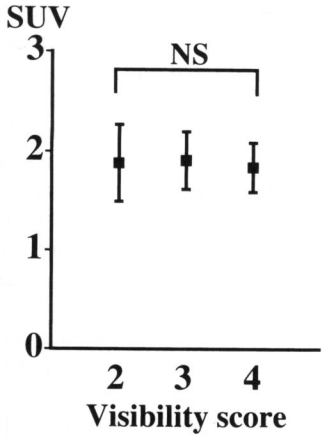

FIG. 2. No significant correlation was obtained between the standardized uptake value and the visibility score (p = 0.801).

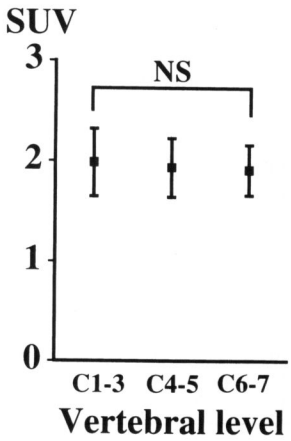

FIG. 3. No significant correlation was revealed between the standardized uptake value and the cervical cord level (p = 0.260).

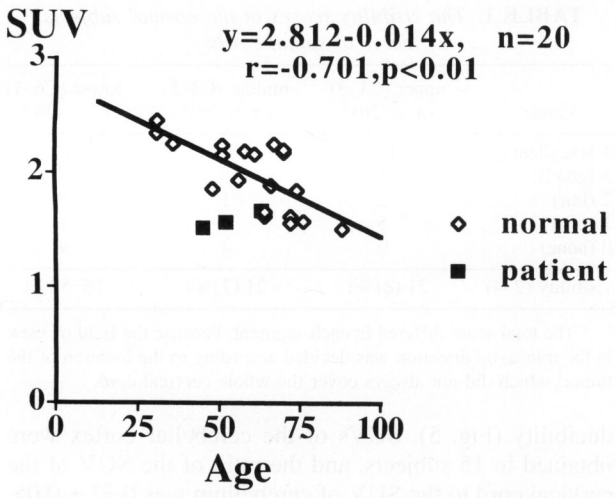

FIG. 4. The relationship between the standardized uptake value (SUV) and the age of the normal subjects (n = 20) and myelopathy patients (n = 3). The SUV showed an age dependency in the normal subjects ($y = 2.812 - 0.014x$; $r = -0.701$, $p < 0.01$). The SUV showed a tendency to decrease in the patients compared with the normal subjects.

mal'' spinal cord because they were all neurologically normal and their MRI or CT did not show any anatomical abnormalities suggestive of a compressive or space-occupying lesion in the spinal canal. Four subjects who underwent a PET study before and after anticancer therapy consisting of a combination of radiation and intraarterial infusion of anticancer drugs showed no change in SUVs in the cervical spinal cord. This is partly because chemotherapeutic agents exert little, if any, direct effect on the spinal cord (11) and partly because the radiation field did not include the spinal cord. Therefore, the effects of non-CNS neoplasms and anticancer therapy were considered negligible in regard to the evaluation of the cervical spinal cord.

Visualization of Entire Cervical Spinal Cord

Metabolic mapping of the spinal cord has rarely been reported in the PET literature. As Di Chiro et al. (4)

TABLE 2. *The metabolic rate for glucose and SUV in normal subjects and myelopathy patients*

Case	Age/Sex	Level of compression	MRGlu (mg/100g/min)	SUV
Normal subjects				
1	71/M	No	2.00	1.80
2	68/F	No	2.27	2.24
3	72/F	No	1.41	1.56
4	51/M	No	2.07	2.24
mean ± SD			1.93 ± 0.37	1.96 ± 0.34
Myelopathy patients				
1	63/M	C3–4	1.80	1.67
2	52/F	C5–6	2.03	1.57
3	45/F	C4–5		1.52
mean ± SD			1.92 ± 0.16	1.59 ± 0.08

No = no compression.

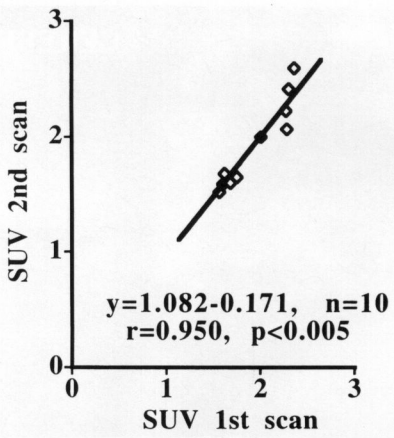

FIG. 5. In the 10 segments of four normal subjects, the standardized uptake value showed good reproducibility between the first and the second scans.

mentioned, this may be partly because the resolution of the scanner was too poor to depict structures as small as the spinal cord and partly due to greater research interest in exploring higher cortical functions by the FDG-PET technique. Recently this situation has changed.

First, the resolution and axial field of view of commercially available PET scanners have been significantly improved. The PET scanner used in the present study was designed for whole-body coverage, with a 15 cm axial direction that can cover the entire cervical cord. It also has high spatial resolution in both the axial and the transaxial directions (almost one-half the diameter of the normal cervical cord), allowing coronal and sagittal reconstruction of images of the cord without loss of resolution. This allowed us to visualize the whole cervical spinal cord.

Second, use of the FDG-PET technique has been extended from the cerebral cortex to the whole body. In the head and neck region, a substantial number of FDG-PET studies on evaluation of neoplastic changes has accumulated (12,13). The visibility of the cervical spinal cord as an anatomical landmark should be established for proper interpretation of head and neck PET studies of neoplasms, because the cervical spinal cord has been described as an excellent internal fiducial marker for anatomical localization of head and neck malignancies with or without co-registration to MRI (14).

Di Chiro et al. (4) used a 15 slice head scanner with low resolution in the axial direction (Neuro-PET) and reported visualization of the upper cervical spinal cord (C1-4) in 10 of 18 (56%) subjects who had no known tumor involvement of the brainstem or cord, but did not rate the visibility. Our multidirectional observation of the cervical cord improved the clarity of visualization in the upper cervical region and extended the visualized area to the inferior end of the cervical spinal cord. The artifact created by the shoulder and subject movement made the inferior region of the cord less clear than the upper cord region, and noise inherent in PET camera and/or reconstruction process still affects the image quality to some

extent. Technical improvements to the PET scanner, such as 3D data collection or newer detectors such as LSO (lutetium oxyorthosilicate) (15), should improve the signal-to-noise ratio. New reconstruction algorithms such as the ordered subset maximal likelihood method (16) are expected to reduce image noise caused by the conventional filtered back-projection method and will probably allow visualization of the thoracic and lumbar cord.

Quantitative Measurement of Glucose Metabolism

In this study glucose utilization was assessed mainly on the basis of SUV. SUV represents a nonkinetic, model-independent quantitative approach based on the assumption of little loss of FDG-6-PO_4 from tissue. There is some controversy regarding the feasibility of SUV, particularly for tumor studies (17). Several factors affect SUV, including body habitus, duration of uptake period, plasma glucose level, and partial volume effect. To minimize the partial volume effect, we used the maximal pixel value within an ROI, which is considered to be the truest measure of actual activity within a small region (17). No correlation was detected between the SUV and the duration of the uptake period in the present study or between SUV and the plasma glucose level within the normoglycemic range. Repeated PET studies in four subjects revealed a constant SUV in the cervical spinal cord. Moreover, in another four subjects who underwent arterial sampling, MRGlu values calculated by the Sokoloff model and SUV were parallel. MRGlu in our study was slightly higher than in Di Chiro's previous report (4), probably due to better resolution of the scanner and different ROI analysis. We therefore consider SUV to be a feasible parameter for evaluating the cervical spinal cord with adequate methods and conditions. The ratio of the SUV of the cord to that of the cerebellar cortex may also be helpful for quantification.

We did not find any correlation between SUV and the cervical cord level. The constant SUV of the cervical cord independent of level is not surprising, since the fundamental structures and the transected areas do not differ significantly across different levels of the cord (7). We found that the SUV of the cervical cord was negatively correlated with subject age. The decrease in glucose utilization with age was more marked than the age-dependent structural atrophy measured by MRI or CT (7). Hence, age-related decreases in SUV may reflect not only decreased cell number but also reduced functional activity.

Finally, we found diffuse metabolic suppression in the presence of focal compression in the myelopathy patients. This suggests chronic circulatory insufficiency of the entire cervical cord caused by venous congestion at the level of compression. Due to the limited number of patients, these are preliminary findings and further investigation is now in progress.

PET is the only method available to assess the metabolic activity of the spinal cord. The present study showed that the cervical spinal cord is clearly visualized by routine FDG-PET and that quantitative assessment of spinal cord metabolism is possible. These preliminary results should be confirmed in normal subjects and patients as further improvements in the PET technique are made.

Acknowledgment: We thank Drs. S. Nishizawa, Y. Magata, K. Ishizu, and H. Okazawa for their support and advice.

REFERENCES

1. Borbely K, Fulham MJ, Brooks RA, Di Chiro G. PET-fluorodeoxyglucose of cranial and spinal neuromas. *J Nucl Med* 1992;33:1931–4.
2. Alavi A, Kramer E, Wegener W, Alavi J. Magnetic resonance and fluorine-18 deoxyglucose imaging in the investigation of a spinal cord tumor. *J Nucl Med* 1990;31:360–4.
3. Higano S, Shishido F, Nagashima M, et al. PET evaluation of spinal cord tumor using ^{11}C-methionine. *J Comput Assist Tomogr* 1990;14:297–9.
4. Di Chiro G, Oldfield E, Bairamian D, et al. Metabolic imaging of the brain stem and spinal cord: studies with positron emission tomography using ^{18}F-2-deoxyglucose in normal and pathological cases. *J Comput Assist Tomogr* 1983;7:937–45.
5. Jabour BA, Choi Y, Hoh CK, et al. Extracranial head and neck: PET imaging with 2-[F-18] fluoro-2-deoxy-*d*-glucose and MR imaging correlation. *Radiology* 1993;186:27–35.
6. Kuhl DE, Metter EJ, Riege WH, Phelps ME. Effects of human aging on patterns of local cerebral glucose utilization determined by the [^{18}F]fluorodeoxyglucose method. *J Cereb Blood Flow Metab* 1982;2:163–71.
7. Suzuki M, Shimamura T. Morphological study of the axial view of the cervical spinal cord by MRI images. *J Jpn Orthop Assoc* 1994; 68:1–13.
8. DeGrado TR, Turkington TG, Williams JJ, Stearns CW, Hoffman JM, Coleman RE. Performance characteristics of a whole-body PET scanner. *J Nucl Med* 1994;35:1398–406.
9. Phelps ME, Huang SC, Hoffman EJ, Selin C, Sokoloff L, Kuhl DE. Tomographic measurement of local cerebral glucose metabolic rate in humans with (F-18)2-fluoro-2-deoxy-*d*-glucose: validation of method. *Ann Neurol* 1979;6:371–88.
10. Huang SC, Phelps ME, Hoffman EJ, Sideris K, Selin CJ, Kuhl DE. Noninvasive determination of local cerebral metabolic rate of glucose in man. *Am J Physiol* 1980;238:E69–82.
11. Okada J, Yoshikawa K, Imazeki K, et al. Change of cerebral glucose metabolism by antineoplastic drug. *Am J Physiol Imag* 1991; 6:162–6.
12. Minn H, Paul R, Ahonen A. Evaluation of treatment response to radiotherapy in head and neck cancer with fluorine-18 fluorodeoxyglucose. *J Nucl Med* 1988;29:1521–5.
13. Bailet JW, Abemayor E, Jabour BA, Hawkins RA, Ho C, Ward PH. Positron emission tomography: a new, precise imaging modality for detection of primary head and neck tumors and assessment of cervical adenopathy. *Laryngoscope* 1992;102:281–8.
14. Uematsu H, Sadato N, Yonekura Y, et al. FDG uptake in normal extracranial head and neck structures: three dimensional approach with high resolution PET. *J Nucl Med* 1996;37:251.
15. Melcher CL, Shweizer JS. A promising new scintillator: cerium-doped lutetium oxyorthosilicate. *Nucl Instr Methods* 1992;314: 212–4.
16. Hudson H, Larkin R. Accelerated image reconstruction using ordered subsets of projection data. *IEEE Trans Med Imag* 1994;13: 601–9.
17. Keyes JW. SUV: standard uptake or silly useless value? *J Nucl Med* 1995;36:1836–9.